Received: 18 November 2020 | Revised: 15 April 2021 | Accepted: 28 April 2021

DOI: 10.1111/psyp.13849

ORIGINAL ARTICLE

PSYCHOPHYSIOLOGY SPR WILEY

Threat imminence modulates neural gain in attention and motor relevant brain circuits in humans

Javier de Echegaray[1,2] | **Stephan Moratti**[1,2,3]

[1]Department of Experimental Psychology, Complutense University of Madrid, Madrid, Spain

[2]Laboratory of Cognitive Neuroscience, Center for Biomedical Technology, Polytechnic University of Madrid, Madrid, Spain

[3]Laboratory of Clinical Neuroscience, Center for Biomedical Technology, Polytechnic University of Madrid, Madrid, Spain

Correspondence
Stephan Moratti, Departamento de Psicología Experimental, Facultad de Psicología, Universidad Complutense de Madrid, 28223 Pozuelo de Alarcón (Madrid), Spain.
Email: smoratti@ucm.es

Funding information
Secretaría de Estado de Investigación, Desarrollo e Innovación, Grant/Award Number: PSI2014-52205-R; Universidad Complutense de Madrid

Abstract

Different levels of threat imminence elicit distinct computational strategies reflecting how the organism interacts with its environment in order to guarantee survival. Thereby, parasympathetically driven orienting and inhibition of on-going behavior in post-encounter situations and defense reactions in circa-strike conditions associated with sympathetically driven action preparation are typically observed across species. Here, we show that healthy humans are characterized by markedly variable individual orienting or defense response tendencies as indexed by differential heart rate (HR) changes during the passive viewing of unpleasant pictures. Critically, these HR response tendencies predict neural gain modulations in cortical attention and preparatory motor circuits as measured by neuromagnetic steady-state visual evoked fields (ssVEFs) and induced beta-band (19–30 Hz) desynchronization, respectively. Decelerative HR orienting responses were associated with increased ssVEF power in the parietal cortex and reduced beta-band desynchronization in pre-motor and motor areas. However, accelerative HR defense response tendencies covaried with reduced ssVEF power in the parietal cortex and lower beta-band desynchronization in cortical motor circuits. These results show that neural gain in attention- and motor-relevant brain areas is modulated by HR indexed threat imminence during the passive viewing of unpleasant pictures. The observed mutual ssVEF and beta-band power modulations in attention and motor brain circuits support the idea of two prevalent response tendencies characterized by orienting and motor inhibition or reduced stimulus processing and action initiation tendencies at different perceived threat imminence levels.

1 | INTRODUCTION

Whenever an individual encounters an aversive event signaling or representing a potential danger, there is a need for highly adaptive behaviors that adequately handle this situation in order to increase the probability of survival. However, such responses are not only stereotyped behavioral patterns based on hard-wired neural populations. Depending on threat imminence these responses can be located onto a continuum spanning from flexible behaviors that ensure adequate sensory analysis of the environment in order to elaborate more efficient action plans, up to hard-wired reflexive responses in circa-strike situations (Fanselow, 1994; Fanselow & Lester, 1988; Mobbs et al., 2009). When threat imminence is low, such as in

pre-encounter situations, increased action planning based on the analysis of new environmental cues updating the individual's actual model of its surrounding is probably the most efficient way to optimize future encounters with potential danger. In post-encounter situations, freezing behaviors are optimal in order not to be detected by a potential predator. During freezing, increased information processing may still be maintained. These processes have been referred to as model-based computations in low to mediate threat imminence situations. Finally, during high threat imminence such as circa-strike situations, reflexive species-specific fight-flight behaviors probably ensure the best survival strategy (Bolles, 1970). This process has been associated with model-free computations in high threat imminence situations (for a detailed review see Mobbs et al., 2020). In the animal literature, it has been consistently shown, that on a continuum of threat imminence such different defense modes emerge, whereby freezing as a form of behavioral inhibition and orienting accompanied by parasympathetically dominated HR deceleration and fight-flight responses associated with sympathetically driven (accompanied by the inhibition of the parasympathetic system) HR acceleration can be localized at low to mediate threat imminence levels and circa-strike situations, respectively (for a detailed review see Roelofs, 2017). Therefore, HR response patterns have been used as a good proxy for perceived threat imminence also in humans (Haagenars et al., 2015; Rössler & Gamer, 2019; Vieira et al., 2020).

Critically, it has been theorized that model-based and model-free computations rely on different neural populations in cortical attention and limbic-brainstem systems that mediate attention and flight-fight responses, respectively (Mobbs et al., 2007; Perusini & Fanselow, 2015; Pourtois et al., 2006). In rodents, different neural populations supporting post-encounter and circa-strike behaviors can be found even in the same structure, for example, the ventral and dorsolateral periaqueductal gray, respectively (Fanselow, 1994). However, model-based computations in low threat imminence situations can update and optimize model-free-related behaviors to be applied in circa-strike moments (Mobbs et al., 2020).

Viewing unpleasant pictures in an experimental setting probably resembles a low threat imminence post-encounter phase in humans, as picture viewing is not a circa-strike encounter with the aversive scene (e.g., viewing of mutilation or attack scenes). However, the degree to which computational strategy (model-based and model-free) will be applied by each individual probably may vary between subjects due to many influences such as experience, genetic and epigenetic factors (Moratti et al., 2015). Experience-related age effects on valence and arousal have been consistently reported (Gavazzeni et al., 2008; Grühn & Scheibe, 2008) and should be taken into account as possible confounds when analyzing response tendencies at behavioral and physiological levels. In general, low threat imminence viewing of unpleasant pictures is normally characterized by parasympathetically dominated sustained HR deceleration, which is believed to reflect increased orienting and stimulus processing (Bradley et al., 2012; Graham & Clifton, 1966; Lacey & Lacey, 1980; Lang et al., 1997). However, Codispoti and De Cesarei (2007) reported that the image size of unpleasant emotional scenes modulated sympathetically driven skin conductance responses (SCRs) but not parasympathetically dominated orienting responses in healthy volunteers. More extreme differences of perceived (psychological) proximity can be observed when these unpleasant pictures contain phobic-related contents. Individuals suffering from a related phobia accelerate rapidly their HR as a response to these images (Hare & Blevings, 1975; Sanchez-Navarro et al., 2018; Weerts & Lang, 1978), indicating the activation of the sympathetic branch of the autonomic nervous system and engaging in model-free behaviors. In non-pathologic healthy participants, these differences may also exist, but are probably more attenuated. These varying predispositions may be expressed as a variance of response tendencies (Hamm & Vaitl, 1996; Hare, 1972; Hare & Blevings, 1975; Hodes et al., 1985; Moratti et al., 2006). Therefore, the analysis of response systems during potential threat or aversion should not only emphasize finding highly consistent responses across individuals at the group level, but should also take into account inter-subject variability.

For example, increased rhythmic neural entrainment to visual complex unpleasant scenes as indexed by steady-state visual evoked field or potential (ssVEF/ssVEP) modulations as recorded with Magnetoencephalography (MEG) or Electroencephalography (EEG), respectively, has been demonstrated consistently in the literature (Keil et al., 2003, 2005, 2009; Moratti et al., 2004, 2008, 2015). However, there is considerable ssVEF inter-subject variability that can culminate in an absence of an emotional arousal modulation of ssVEF responses in pathologies such as major depression (Moratti et al., 2008, 2015). In healthy subjects, peripheral indexes of model-based or model-free computations such as HR and SCR modulations may help to explain inter-individual differences in ssVEP/ssVEF modulations in cortical sensory or attention systems.

For example, increased oscillatory evoked responses in the visual system to luminance-modulated emotional pictures covary with sympathetic ANS activation (Keil et al., 2008) and parasympathetic dominated orienting responses (Moratti et al., 2004) probably indicating different degrees of interleaved model-free and model-based computations during the viewing of emotional pictures. However, Moratti et al. (2004) only showed increased HR deceleration for unpleasant emotional pictures together with increased ssVEF responses in visual and frontoparietal attention circuits at a group level. No direct relationship

between these two response systems has been tested so far (e.g., no regression of the ssVEF responses by HR deceleration was assessed in that report).

In the present study, we focus on inter-subject variability at distinct response levels in healthy humans in order to characterize inter-individual differences of threat imminence during the viewing of unpleasant and neutral pictures. Thereby, HR change differences between unpleasant and neutral pictures will serve to index the degree to which the sympathetic and parasympathetic branch of the autonomic nervous system dominates during unpleasant picture viewing for an individual participant. We present our hypotheses and findings in a general framework that the tendency to accelerate or decelerate HR responses to unpleasant pictures reflects inter-individual differences in applying a model-free or model-based encounter strategy, respectively (Haagenars et al., 2015; Rössler & Gamer, 2019; Vieira et al., 2020). Critically, we assess how the variability in the encounter strategy as indexed by HR changes biases activity modulations in visual-attentional and motor preparatory cortical networks.

First, sensory gain modulations in visual and attentional cortical circuits will be quantified by ssVEF responses evoked by and phase-locked to flickering unpleasant and neutral complex scenes taken from the International Affective Picture System (IAPS; Lang et al., 2005). Steady-state response modulations by emotion are a robust and well-replicated finding (see above). However, here we will assess in which cortical circuits, that are driven by flickering emotional pictures, HR change patterns explain a significant amount of ssVEF variance by fitting linear models in cortical source space. We hypothesize that stimulus-locked ssVEF modulations in occipital and parietal cortical visual attention systems (Corbetta et al., 2008; Pourtois et al., 2006) will covary with the degree of model-based orienting responses as indexed by a parasympathetically dominated HR deceleration (Bradley et al., 2012; Graham & Clifton, 1966; Lacey & Lacey, 1980).

As orienting has been associated with attentional immobility (Roelofs, 2017), we hypothesize that cortically localized MEG/EEG beta-band desynchronization (15 to 35 Hz) as a marker of premotor and motor cortex excitability (Lachert et al., 2017; Park et al., 2013; Pfurtscheller & Aranibar, 1979; Pfurtscheller & Lopes da Silva, 1999; Tzagarakis et al., 2015) will also covary with HR change differences. Thereby, beta-band desynchronization should be reduced during model-based orienting as indexed by HR deceleration, whereas model-free strategies accompanied by HR acceleration should covary with increased beta-band desynchronization. Interestingly, HR acceleration together with beta-band desynchronization has been observed during mental imagery of action initiation (Pfurtscheller et al., 2013), whereby accelerative HR change patterns have been associated with early stages of mental representations of action initiation (Jennings & Woods, 1977; Jennings & Van der Molen, 2005; Jennings et al., 1990; Pfurtscheller et al., 2013; Roelofs, 2017).

Although our study does not address direct heart-brain interactions (e.g., ssVEFs are phase locked to the visual stimuli and induced beta-band activity is not within the 4 Hz to 7 Hz theta band range where inter-trial neuro-cardiac coherence is observed see Park et al., 2018), model-based orienting and model-free action initiation tendencies can also be conceptualized within the neuro-visceral integration model (for detailed reviews see Schwerdtfeger et al., 2020; Thayer & Lane, 2009; Tumati et al., 2021). In this model, the prefrontal cortex tonically inhibits the central nucleus of the amygdala that regulates via subcortical and brainstem structures autonomic responses. Critically, this model assumes that the prefrontal cortex becomes hypoactive under stress and high levels of threat imminence resulting in a decrease of the tonic inhibition of the amygdala mediated cardioacceleratory subcortical threat circuits (Thayer, 2006). This disinhibition of sympathoexcitatory circuits mobilizes the necessary energy for the flight-fight response and is characterized by HR acceleration. This situation maps onto the above described circa-strike situations calling for model-free immediate action. We hypothesize that under these circumstances excitability of the motor cortex should be high as reflected by increased beta-band desynchronization in the premotor and motor cortex. However, at low threat imminence levels, the prefrontal cortex as part of the attention system (Corbetta et al., 2008) exerting cognitive control should be highly active and the cardioacceleratory circuit should be inhibited resulting in parasympathetically dominated HR decrease as observed during the orienting response facilitating sensory processing and motor inhibition. This scenario would map onto model-based computational strategies accompanied by increased ssVEF responses in visual-attention networks and decreased beta-band desynchronization in premotor and motor cortex as outlined above.

2 | METHOD

2.1 | Subjects

Forty-three healthy volunteer participants (34 right-handed females, 9 right-handed males. Mean age = 25.4; range 18 to 55 years) participated in the study after given written informed consent and psychological screening. All participants were previously evaluated in order to be categorized as healthy control subjects and had not been exposed to pictures from the International Affective Picture System (IAPS) before. Screening consisted of applying the Hamilton Anxiety Rating Scale (HARS), Hamilton Depression Rating Scale (HDRS), General Health Questionnaire (GHQ-28), and DSM-IV SCID before MEG

recording. Subjects were considered healthy when (i) they did not meet DSM-IV criteria for any mental illness and scoring below 8 in the HDRS, below 18 in the HARS, and did not exceed 24 points in the GHQ-28. All subjects had a normal or corrected-to-normal vision. The study had full ethical approval from the local ethics committee. The study is part of an ongoing clinical project (TEMPACOR), but here we only report data of healthy participants testing the aforementioned hypothesis related to the processing of unpleasant and neutral pictures.

2.2 | Stimuli and Procedure

Sixty colored pictures[1] were selected from the IAPS (Lang et al., 2005) according to normative arousal and valence dimensions, resulting in 20 unpleasant (ten mutilation and ten attack scenes), 20 pleasant (ten erotic couples and ten familiar scenes) and 20 neutral images (10 household and 10 neutral person scene). Mean normative valence ratings on a 9-point scale were 2.76 ± 0.19 for unpleasant, 4.87 ± 0.05 for neutral, and 7.33 ± 0.13 for pleasant pictures. Mean normative arousal ratings were 6.9 ± 0.07, 2.8 ± 0.13 and, 5.44 ± 0.24, respectively. Accordingly, participants' ratings were highly similar to the normative ratings (valence: 2.05 ± 0.48 for unpleasant, 5.21 ± 0.34 for neutral, and 7.21 ± 0.91 for pleasant pictures; arousal: 7.62 ± 0.61 for unpleasant, 4.39 ± 0.19 for neutral, and 5.48 ± 1.37 for pleasant pictures). Selected stimuli did not differ in brightness, contrast, nor color spectra between categories (see Moratti et al., 2004). However, as mentioned above, here we only report on the processing of unpleasant and neutral pictures.

Visual stimuli were presented in a magnetically shielded chamber by a video projector (Panasonic PT-D7700E) via a mirror system, subtending a 10º visual angle, both vertically and horizontally. Participants were instructed to fixate to a centered fixation cross (visual angle 1.6º vertically and horizontally) that was presented throughout the whole experiment during picture presentation. Stimuli were presented in a pseudorandom order (pictures of the same category were not presented more than twice in a row). Each trial consisted of a 6 s presentation of one picture in a luminance-modulated mode of 10 Hz, resulting in 60 on-off cycles of 0.05 s each. Intertrial intervals varied randomly from 8 s to 12 s.

Subjects performed a passive viewing task whereby 60 images were pseudorandomly presented during the experimental session, divided in two experimental blocks of 20 min. Each picture was presented twice (once per block but within a different order in each block) resulting in 120 trials. As we report here data for the unpleasant and neutral conditions only, 80 trials entered in the current analysis. After the MEG recording and outside the MEG chamber participants were asked to rate the previously presented stimuli according to valence and arousal dimensions using a computerized Self-Assessment Manikin Scale (SAM; Lang et al., 2005).

[1]The IAPS picture numbers were: 1050 1120 1201 1300 1930 2050 2070 2080 2160 2165 2170 2190 2200 2210 2230 2311 2340 2341 2360 2381 2440 2480 2570 2850 3000 3010 3053 3060 3071 3080 3102 3110 3130 3530 4650 4651 4652 4658 4659 4660 4664 4670 4680 4690 6260 6350 6510 6540 7002 7009 7010 7020 7030 7040 7080 7175 7233 7235 9070 9405.

2.3 | Data acquisition and preprocessing of MEG data

MEG data of 31 participants were recorded at the Laboratory for Cognitive and Computational Neuroscience, at the Center for Biomedical Technology (CTB, Madrid, Spain). The MEG was recorded continuously at a rate of 600.00 Hz (on-line band-pass filter of 0.1-200Hz), using a 306 channels whole-head system (VectorView© Elekta Neuromag Oy, Helsinki, Finland 2005). For artifact monitoring, the electrooculogram (EOG) was recorded with electrodes attached above, below, left to, and right to the outer canthus. The electrocardiogram (ECG) for heart rate assessment was recorded with electrodes placed at the left mid-clavicle and lower right rib bone. Additionally, one electrode was attached to the left earlobe serving as the ground electrode. EOG and ECG were recorded simultaneously using standard Au electrodes (NSC Electromedicina). EOG and ECG were recorded using the same sample frequency and online filters as the MEG data.

Twelve of the forty-three participants were previously recorded using a 148-channel whole-head system (Magnes 2500 WHS, 4-D Neuroimaging, San Diego, USA). Data of these subjects have been published in a previous study (Moratti et al., 2015). Data of these participants had been recorded at a sample frequency of 254.3 Hz and applying an online filter of 0.1 to 60 Hz. In order to apply the same preprocessing and source localization procedures as in the new sample, data have been up-sampled to 600 Hz using a cascade algorithm as implemented in Brainstorm (https://neuroimage.usc.edu/brainstorm/) using the signal processing toolbox of MATLAB (MathWorks©). However, task, experimental design, psychological evaluation, preprocessing, and source localization (see below) did not differ from the thirty-one subjects that were recorded with the Elekta system. As the Magnes 2500 WHS system is equipped with magnetometers only, only magnetometer data from the Elekta system were considered for further analysis. Ashrafulla et al. (2011) have shown that MEG data from different recording systems are comparable when using the minimum norm estimation for cortical source localization.

Eyeblink and heartbeat noise were corrected by Independent Component Analysis as implemented in the Brainstorm toolbox (ICA-JADE). Noisy trials due to movement artifacts and horizontal eye movements as monitored by the EOG were determined by visual inspection and excluded from the analysis. Then, MEG data were digitally band-pass filtered between 1 and 40 Hz (60 dB stop-band attenuation) before averaging pictures by category (unpleasant and neutral) across the 6 s post-stimulus interval subtracting a 0.5 s pre-stimulus baseline. Finally, the averaged epochs were submitted to a moving-window averaging procedure, in which a 1 s window containing 10 cycles of a 10 Hz oscillation was shifted across the epoch in steps of 0.1 s (see for example Yuan et al., 2018). All preprocessing was performed using the Brainstorm toolbox (Tadel et al., 2011).

2.4 | Cortical source analysis of ssVEF and induced beta-band activity

Cortical source reconstruction was applied to the extracted ssVEF signal using a canonical cortical surface mesh (7001 vertices) from the Montreal Neurological Institute (MNI) phantom brain (Collins et al., 1998). The individual head and sensor positions of each subject were co-registered with the template brain by realigning the individual with the template brain's fiducials and minimizing the mean distance between the individual head shape points and the template brain scalp surface (Moratti et al., 2011). Thereafter, the forward model was calculated by a head model based on overlapping spheres (Huang et al., 1999). Finally, a weighted Minimum Norm Estimation (wMNE; Gramfort et al., 2014) was used to calculate the current density of the ten 10 Hz cycles previously extracted by the moving window averaging procedure (see above) on the cortical surface for later analysis. The 10 Hz power of the ssVEFs at each cortical vertex was extracted by Fast Fourier Transformation (FFT) and $\log_{10}$ transformed. Then, the differences between cortically localized $\log_{10}$ transformed current density maps for unpleasant and neutral pictures were submitted to further statistical analysis (see below). All cortical source localization was performed using the Brainstorm toolbox (Tadel et al., 2011).

The cortical source analysis of induced beta-band activity was based on the same artifact-free trials (−0.5 s pre-stimulus and 6 s post-stimulus interval) as the ssVEF analysis, but without filtering the epochs. In order to obtain cortically localized induced beta-band activity estimates, each single trial of the MEG data was multiplied by the image kernel of the wMNE. Then, the resulting single-trial current density maps were submitted to an FFT for each picture category. The FFT was calculated within a beta-band frequency range of 15 to 35 Hz. However, single-trial source estimation was restricted to a previously defined region of interest (ROI) corresponding to premotor and motor areas of the brain (Brodmann area BA6, see Figure 1) as changes in MEG beta-band activity associated with the excitability of the premotor and motor cortex have been reported for this brain region before (Barratt et al., 2018; Koelewijn et al., 2008; Rossiter et al., 2014). Finally, the resulting FFTs in source space were averaged across trials to obtain a power estimate of induced spectral activity. The resulting power for each spatial location (within the ROI) and frequency bin (15 to 35 Hz) of the unpleasant and neutral picture conditions were $\log_{10}$ transformed and then subtracted from each other for further statistical analysis.

2.5 | Preprocessing of heart rate change data

The heart rate response was monitored and collected by the ECG channel during MEG recording. Additionally, for those subjects for whom technical problems impaired the heart rate recording ($N = 8$), the magnetocardiographic (MCG) signal was extracted from the MEG recording by an

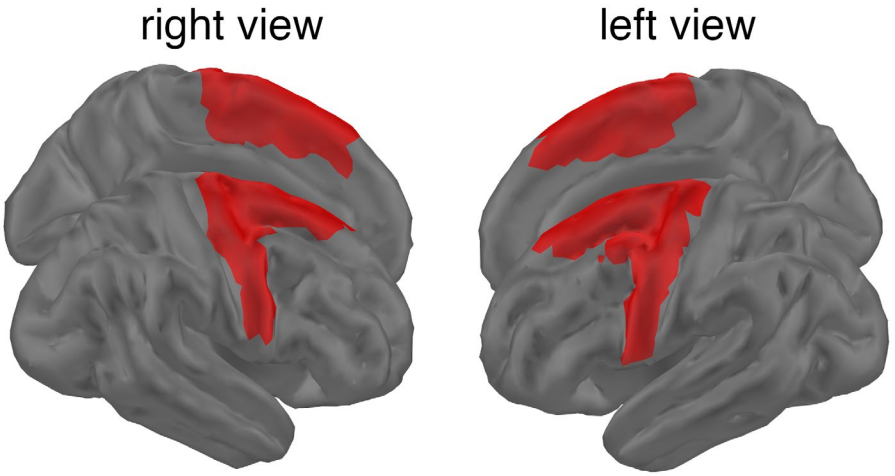

FIGURE 1 Regions of interest (ROI) for the induced MEG beta-band cortical source analysis are shown and correspond to the premotor and motor areas (Brodmann BA6) of the left and right hemispheres.

ICA as implemented in the Brainstorm toolbox (ICA-Jade). For both, the ECG and MCG, inter-beat intervals were determined based on R-peak time intervals from 5 s before and 9 s after stimulus onset. Heart rate (HR) in beats per minutes (bpm) was estimated in 0.5 s steps using weighted averages (Reyes del Paso & Vila, 1998) as implemented in the MATLAB toolbox Kardia (Perakakis et al., 2010; https://sourceforge.net/projects/mykardia/). Finally, HR change was calculated for the 6 s post-stimulus interval subtracting a 2 s baseline for unpleasant and neutral picture content.

2.6 | Statistical analysis of HR change

As in previous reports (Bradley, 2009; Lacey & Lacey, 1980; Sokolov, 1963) differences in HR deceleration for unpleasant and neutral pictures have been greatest after 2 s to 3 s after stimulus onset, mean differences between these two conditions and across this time interval were tested against zero by a one-sample *t* test. Then, subjects were divided into HR accelerators and decelerators depending on their mean HR change (unpleasant – neutral) between the analyzed 2 s to 3 s interval in order to depict the corresponding difference waves.

2.7 | Statistical analysis of emotion modulated cortically localized ssVEFs

Current source density difference maps (unpleasant – neutral) of $\log_{10}$ transformed ssVEF power for each subject were tested against zero at each vertex of the canonical brain surface. To safeguard against false positives due to multiple comparisons, clusters were formed based on these *t* tests with a two-sided cluster threshold of $p = .01$ and having at least two spatially adjacent neighbors. Then, the same procedure was repeated 1,000 times and at each repetition, the current density contrasts (unpleasant – neutral) were permuted with zero current density maps under the Null hypothesis that the differences between unpleasant and neutral ssVEF responses are not different from zero. At each repetition, the biggest t cluster sum entered into a permutation distribution. Only t clusters of the originally observed contrast that formed cluster sums located below the 2.5 percentile or above the 97.5 percentile (two-sided test) of the cluster-based permutation distribution were considered as significant (Nichols & Holmes, 2002). This test was performed using the fieldtrip toolbox (http://www.fieldtriptoolbox.org). For brain vertices of greatest differences, we report the parametric *t* test results with its associated effect size (Cohen's d).

2.8 | Statistical analysis of cortically localized ssVEFs and their relation to HR change

However, one of our main objectives was to relate HR change differences between unpleasant and neutral picture categories to ssVEF modulations by emotion. The same non-parametric cluster-based permutation test as described above was applied, but instead of a one-sample *t* test, a multiple regression model was fitted at each vertex of the canonical brain surface in order to test the relationship between ssVEF contrasts (unpleasant – neutral) and mean HR change differences (unpleasant – neutral) between 2 and 3 s (see above). In order to control for age as a possible confound, age was also introduced as a regressor (see Supplemental Material for details and MATLAB code).

2.9 | Statistical analysis of induced MEG beta-band activity and its relation to HR change

In order to test a linear relationship between induced $\log_{10}$ transformed beta-band power differences (unpleasant – neutral) in premotor and motor areas and HR change differences (unpleasant – neutral between 2 and 3 s after picture onset), the same non-parametric cluster-based permutation statistics was applied as explained in the previous section. Age was also introduced as a regressor in order to control for age as a possible confound. However, the multiple regression model was restrained to the predefined ROI of Brodmann area BA6 (see above) and frequency window. As we expected a negative relationship between beta-band and HR change differences (stronger beta-band desynchronization – stronger HR acceleration; stronger beta-band synchronization – stronger HR deceleration) the *t* statistics for the *b* coefficients were based on a directed one-sided test for HR change. The possible age influence was tested two-sided as no a priori hypothesis for the directionality had been established before.

3 | RESULTS

3.1 | SAM Ratings and HARS scores

On the SAM valence dimension unpleasant images (valence 2.05 ± 0.08 *SEM*) were rated as less pleasant than neutral (valence 5.23 ± 0.05 *SEM*) pictures ($t(38) = -34.05$, $p < .001$, $d = -5.5$). In contrast, arousal ratings were higher for unpleasant (arousal 7.40 ± 0.22 *SEM*) than for neutral (arousal 4.45 ± 0.19 *SEM*) scenes ($t(38) = 9.87$,

$p < .001$, $d = 1.6$). Thus, the SAM ratings after the MEG session were comparable with the normative evaluations (see Method).

With respect to physiological reactivity HR change (mean difference unpleasant – neutral between 2s and 3s after stimulus onset) did not predict valence rating changes (unpleasant – neutral: $t(36) = 1.11$, $p = .275$, $f^2 = 0.03$), whereas age did ($t(36) = -3.82$, $p < .001$, $f^2 = 0.40$, see Figure 2a). The same pattern was observed for the arousal rating changes (unpleasant – neutral); HR change did not predict arousal ratings ($t(36) = -0.96$, $p = .344$, $f^2 = 0.02$), whereas age was associated with higher arousal ratings ($t(36) = 3.39$, $p = .002$, $f^2 = 0.32$; see Figure 2b). However, these effects were mainly driven by the older participants as reflected by the lower effect sizes.

We also tested if anxiety levels, depression scores and age predicted HR change differences introducing these predictors in a multiple regression analysis. Neither HARS scores ($t(39) = 0.99$, $p = .340$, $f^2 = 0.02$), HDRS scores ($t(39) = -0.95$, $p = .346$, $f^2 = 0.02$), nor age ($t(39) = 1.44$, $p = .159$, $f^2 = 0.05$) were associated with HR changes.

3.2 | Cortically localized ssVEF response modulation across all participants

First, we will report group results ignoring inter-individual differences in physiological reactivity in order to replicate previous findings. Figure 3a depicts two clusters of contrasts between unpleasant and neutral pictures of cortically localized ssVEF power (left cluster: summed t values = 1,563, $p = .002$, maximum $t(42) = 6.02$, $p < .001$, $d = 0.93$; right cluster: summed t values = 1,195.8, $p = .002$, maximum $t(42) = 5.96$, $p < .001$, $d = 0.92$). Unpleasant pictures elicited increased ssVEF responses in comparison to neutral scenes in source clusters spanning the left and right primary visual cortex, right ventral temporal cortex and left occipito-parietal cortex. However, 7 out of 43 participants (16%) did not show increased ssVEFs for unpleasant pictures in the visual cortex (Figure 3b).

3.3 | HR change across all subjects

As performed with ssVEF power changes, here we first report group results of HR changes evoked by unpleasant and neutral images. As has been shown in previous reports (Moratti et al., 2004), triphasic HR changes were characterized by an initial deceleration, a subsequent acceleration, and a final deceleration. However, unpleasant pictures elicited a stronger initial deceleration than neutral images (see Figure 4a; mean contrast unpleasant – neutral between 2s and 3s: $t(42) = 2.14$, $p = .038$, $d = 0.33$). At a group level, we observed the typical "fear" bradycardia for unpleasant pictures in humans (Bradley et al., 2001). However, the effect size of HR bradycardia for unpleasant pictures is rather small and the 95% confidence interval almost includes zero (Figure 4b). As can be seen in Figure 4b,a considerable number of participants were characterized by HR acceleration for unpleasant pictures (16 out of 43 participants corresponding to 37.21%). Figure 4c shows the HR change difference waves for accelerators and decelerators. There were no baseline differences between decelerators and accelerators for unpleasant (decelerators 71.6 bpm ±2.51 SEM; accelerators 69.1 bpm ± 2.57 SEM; $t(41) = 0.69$, $p = .502$, $d = 0.21$) and neutral pictures (decelerators: 71.2 bpm ±2.58 SEM; accelerators 69.5 bpm ±2.51 SEM; $t(41) = 0.44$, $p = .661$, $d = 0.14$).

3.4 | Cortically localized ssVEF response modulation explained by HR change

Heart rate change differences (mean difference unpleasant – neutral between 2s and 3s after stimulus onset) and age were entered in a multiple regression model in order to explain power differences between cortically localized ssVEF responses for unpleasant and neutral pictures (see Method). Considering the two regressors, HR change differences and age did not correlate ($r = 0.24$, $p = .114$, 95% CI [−0.06 0.51]).

The non-parametric cluster-based permutation test did not yield any cluster explaining significant variance of ssVEF modulation by age (maximum summed t value = 235.7, $p = .04$, no negative cluster). However, in left and right parietal clusters variance of emotional ssVEF power modulations was explained by HR change (Figure 5a; left cluster: summed t value = −659.65, $p = .006$, minimum t (40) = −4.53, $p < .001$, $f^2 = 0.51$; right cluster: summed t value = −363.67, $p = .025$, minimum t (40) = −4.59, $p < .001$, $f^2 = 0.52$). Both negative clusters indicate that increasing ssVEF power differences between unpleasant and neutral stimuli were associated with greater HR deceleration for unpleasant pictures (Figure 5b).

3.5 | Induced MEG beta-band activity in premotor and motor areas covarying with HR change

With respect to the linear model with HR change and age as regressors and induced FFT power differences (unpleasant – neutral) of premotor and motor areas (see Method) as a dependent variable, the non-parametric cluster-based permutation statistics revealed a significant frequency by spatial location cluster in the beta-band (19.2 Hz to 19.5 Hz: summed t value = −841.82 $p = .03$, Figure 6a,b). Although the two clusters in the left and right hemisphere were connected by

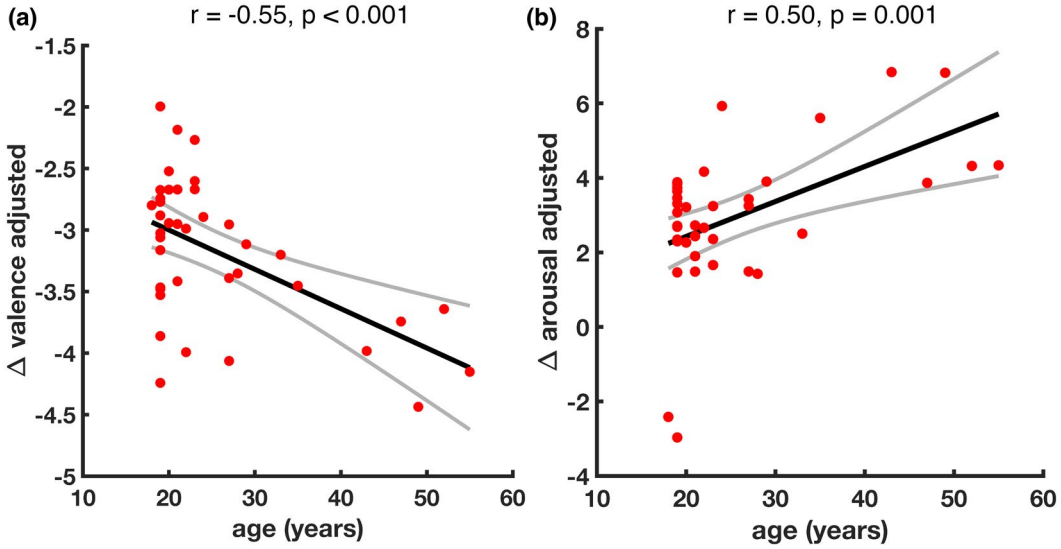

FIGURE 2 Age predicts valence and arousal rating changes (unpleasant – neutral). (a) Adjusted (by HR changes) valence rating changes indicate that unpleasant stimuli are rated more negatively with age. (b) Adjusted (by HR changes) arousal rating changes increase with age. The red dots represent individual data points. The black line indicates the regression slope, whereas the grey lines depict the 95% confidence kernel density. The correlation coefficients estimate the linear relation between the adjusted valence and arousal rating changes and age.

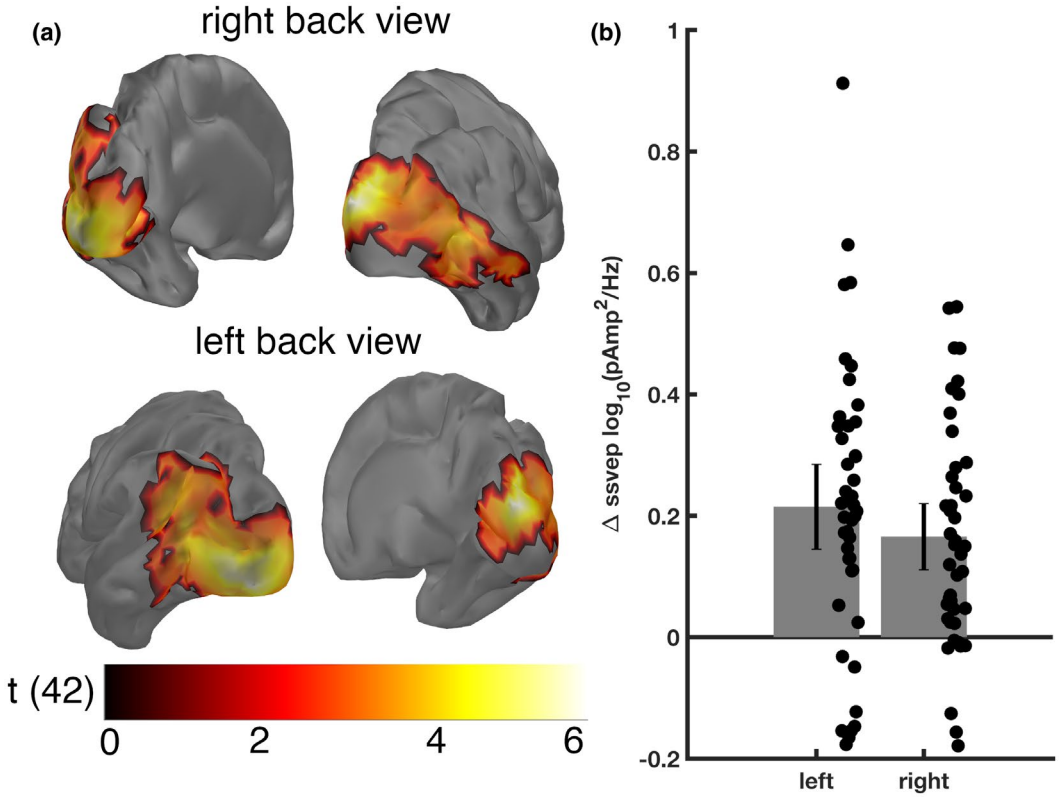

FIGURE 3 Unpleasant emotional scenes evoke increased ssVEP power compared to neutral picture content. (a) Non-parametric cluster-based permutations testing the difference between ssVEF power for unpleasant and neutral pictures against zero depicts two clusters (summed t values >1,563, $p = .002$) of ssVEF power modulations by emotion. The colorbar indicates the t values. (b) Bar plots of group mean differences between ssVEF power for unpleasant and neutral pictures derived from the surface vertices with the maximum t value (see main text) of the left and right clusters are shown. The error bars depict the 95% confidence intervals of mean differences. The scatterplot depicts the individual ($N = 43$) ssVEF power differences. Note, that around 16% of subjects did not increase ssVEF power for unpleasant pictures in the occipital and parietal cortex

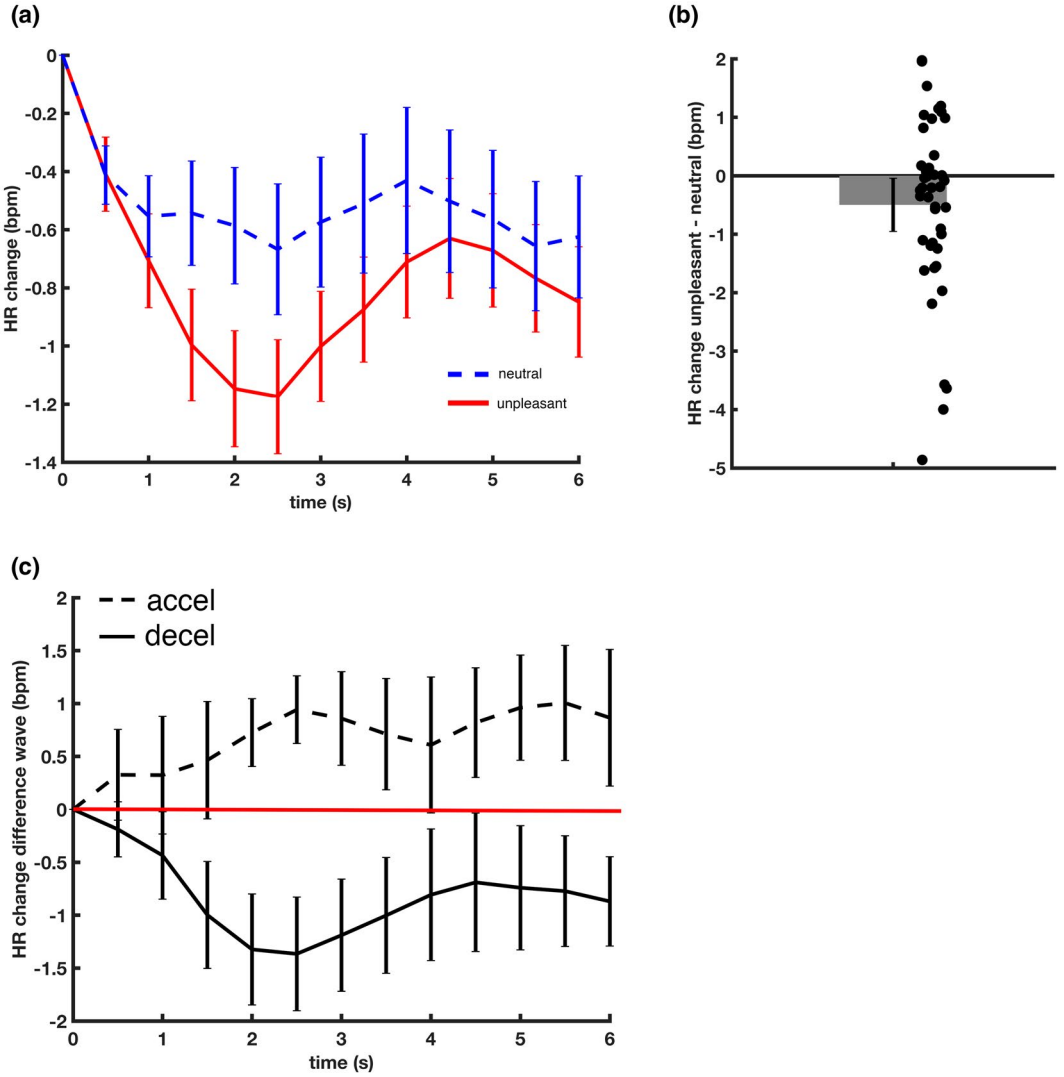

FIGURE 4 HR change for unpleasant and neutral pictures are shown. (a) HR change for unpleasant and neutral pictures across 6 s of picture viewing is depicted. The error bars correspond to between-subject standard errors. (b) The mean HR difference for unpleasant and neutral pictures between 2 and 3 s is shown in the bar plot. The error bar indexes the 95% confidence interval of the mean difference. The scatterplot shows HR change differences for individual participants. Note that 37.21% of the sample actually accelerated their HR during unpleasant picture viewing, although the statistics at the group level indicate a general HR deceleration. (c) Difference waves (unpleasant – neutral) for accelerators (mean 2s – 3s HR change greater than zero) and decelerators (mean 2s – 3s HR change smaller than zero) are depicted. The red line represents the zero line. The error bars indicate the 95% confidence interval of the difference waveforms

the frequency domain, we report the minimum t values of the model fit for each hemisphere (left cluster minimum $t(40) = -4.15$, $p < .001$, $f^2 = 0.43$; right cluster minimum $t(40) = -4.75$, $p < .001$, $f^2 = 0.56$). The cluster indicated a negative relationship between induced beta-band activity modulations (unpleasant – neutral) and HR change differences (unpleasant – neutral) in left and right premotor and motor brain areas (Figure 6b). Heart rate acceleration for unpleasant pictures were related to beta-band desynchronization, whereas greater HR deceleration induced stronger synchronization (less beta-band desynchronization) in that frequency band (Figure 6c,d). Only HR change added significant variance to the model estimation, whereas age did not (positive cluster summed t value = 26.15, $p = .981$; negative cluster summed t value = −86.35, $p = .706$).

However, as the relationship between induced beta-band activity and HR change were also negatively related as observed for the association between ssVEF power and HR change, we were concerned that our beta-band observations resulted from frequency or spatial leakage of the first harmonic of the stimulus flicker frequency (20 Hz). To safeguard against such an explanation for the induced beta-band results, the same non-parametric cluster-based permutation statistics as for the beta-band range were repeated. However, this

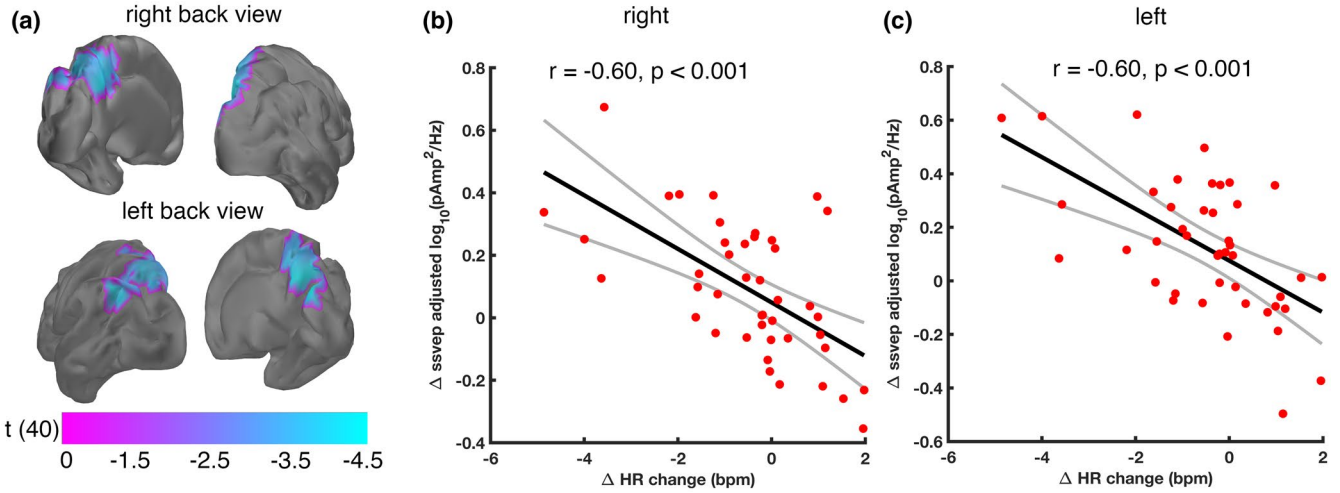

FIGURE 5 Greater HR deceleration for unpleasant pictures is linearly related to increased ssVEF power in the left and right parietal cortex. (a) Left and right clusters in which HR changes explain a significant variance of emotional stimulus locked ssVEF power modulation are shown (summed t values <-363.67, $p < .025$). The colorbar indicates the t values of the HR coefficient tested against zero. (b) Scatterplots of adjusted (by age) $\log_{10}$ transformed ssVEF power changes (unpleasant – neutral) in relation to HR changes (unpleasant – neutral) for the source vertices of the minimum t values of the left and right clusters are shown, respectively. The red dots represent individual data points. The black line indicates the regression slope for the adjusted (by age) data, whereas the grey lines depict the 95% confidence kernel density. The correlation coefficients estimate the linear relation between the adjusted ssVEP power and HR changes

time the frequency range was restricted to a range between 19.9 Hz and 20.1 Hz in order to encompass 20 Hz. No significant negative clusters emerged (cluster with lowest p value summed t value $= -8.06$, $p = .343$). Further, the adjusted $\log_{10}$ transformed 20 Hz power changes in the source vertices of the minimum t values for the left and right clusters derived from the beta-band analysis before, did not correlate with HR changes (Figure 6e,f).

3.6 | Induced premotor and motor MEG beta-band activity and evoked parietal ssVEF response modulations

In order to assess if participants that showed increased induced beta-band desynchronization also showed less evoked ssVEF power modulations by unpleasant pictures and vice versa, beta-band and ssVEF activity changes at vertices that best fitted to HR changes were collapsed across the left and right hemispheres and correlated between each other. As can be seen in Figure 7, increased neural gain in parietal brain regions as indexed by augmented ssVEF power was associated with decreased cortical excitability in premotor and motor areas as indexed by induced beta-band synchronization. In contrast, subjects that suppressed ssVEF power for unpleasant pictures were characterized by increased beta-band desynchronization (cortical excitability) in premotor and motor areas during unpleasant picture viewing ($r = 0.44$, $p = .003$, 95% CI [0.16 0.65]).

4 | DISCUSSION

Here, we show that distinct levels of threat imminence during emotional picture viewing in humans as indexed by different HR response patterns are associated with differential neural gain control in attention and motor-relevant cortical regions. Critically, parasympathetically dominated fear bradycardia (HR deceleration) as an index of model-based computational strategies such as increased attention and sensory processing (Bradley et al., 2012; Graham & Clifton, 1966; Lacey & Lacey, 1980; Lang et al., 1997) during the viewing of unpleasant pictures was linearly related to an increase of ssVEF responses in parietal cortex. Enhanced ssVEF responses have been associated with increased neural gain in visual and attentional brain circuits facilitating the processing of visual input (Keil et al., 2005; Moratti et al., 2004). The increased processing of visual information may also give rise to increased cognitive control and emotion regulation as these processes have been associated with model-based computations (see Mobbs et al., 2020). Within the framework of the neuro-visceral integration model these cognitive functions have been associated with prefrontal activity inhibiting subcortical cardioaccelerative circuits via the amygdala (Thayer, 2006; Thayer & Lane, 2009) giving raise to parasympathetically dominated HR deceleration as observed during orienting responses. Consistent with motor inhibition during orienting (Roelofs, 2017), HR deceleration covaried with reduced beta-band desynchronization in pre-motor and motor cortex reflecting a neural gain decrease in action initiation

networks. In line with our results, increased attention to unpleasant stimuli has been associated with attentive immobility and modulation of motor cortex activity by brain circuits such as the amygdala and the periaqueductal gray in humans (Hermans et al., 2013; Sagaspe et al., 2011).

In contrast, HR acceleration that indexes defense response preparation reflecting model-free computational strategies for higher threat imminence levels was accompanied by reduced ssVEF responses in the parietal cortex for high arousing unpleasant pictures. However, greater accelerative HR

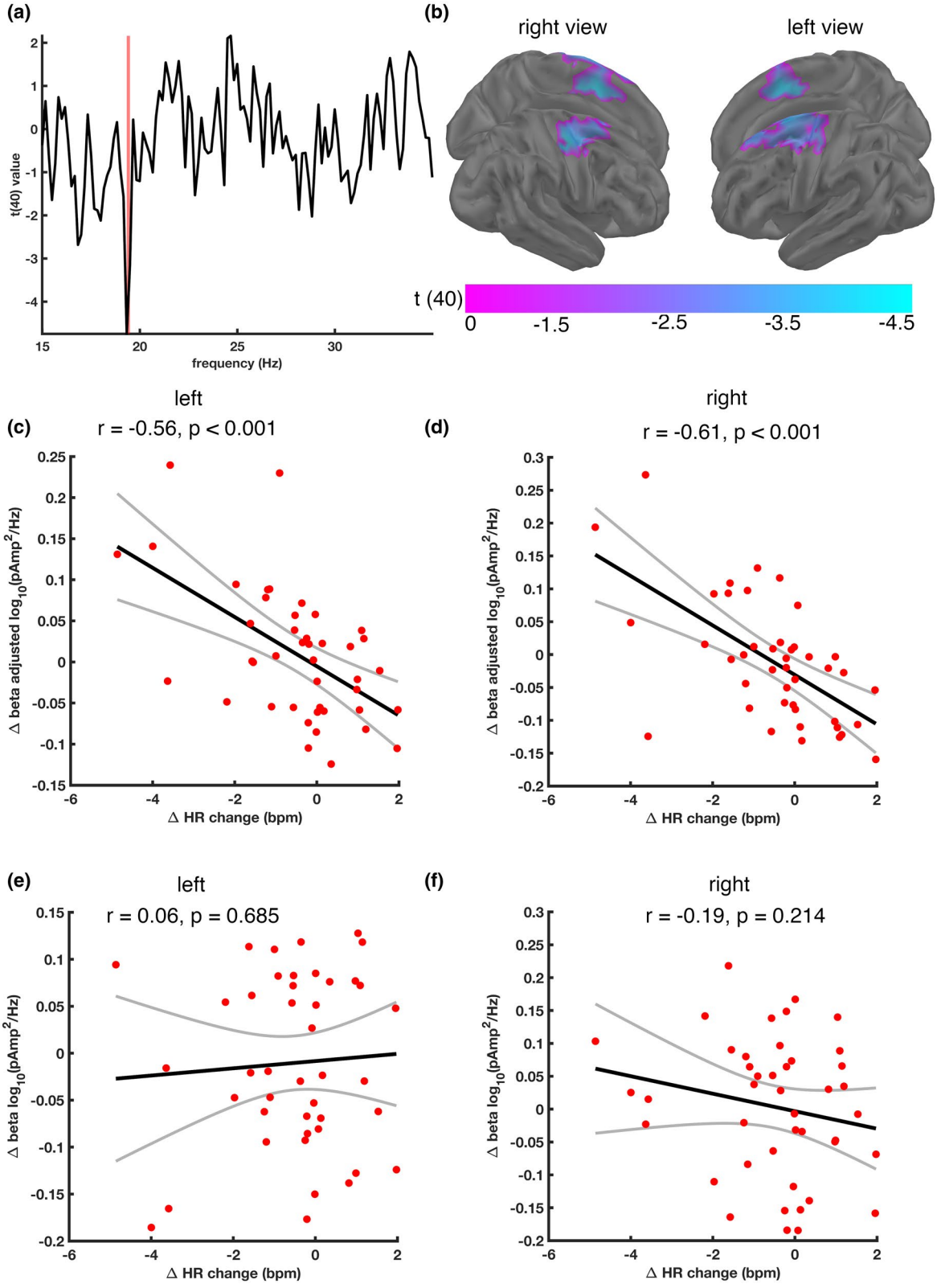

FIGURE 6 HR change difference (unpleasant – neutral) is linearly related to beta-band activity differences (unpleasant – neutral) in premotor and motor cortices. (a) Non-parametric permutation statistics resulted in a frequency by spatial location cluster (summed t value = −841.82 $p = .03$). The figure shows the t values for the most significant location by frequency bins. The red bar indicates the significant cluster between 19.2 and 19.5 Hz. Note that this frequency range is just below the 20 Hz harmonic of the 10 Hz stimulus flicker. (b) The localization of this cluster extended across the left and right premotor and motor ROIs. The colorbar indicates the t values of the HR coefficient tested against zero. (c and d) Scatterplots of adjusted (by age) $\log_{10}$ transformed beta-band power changes (19.2–19.5 Hz) in relation to HR changes for the source vertices of the minimum t values for the left and right clusters are shown, respectively. The red dots represent individual data points. The black line indicates the regression slope for the adjusted (by age) data, whereas the grey lines depict the 95% confidence kernel density. The correlation coefficients estimate the linear relation between the adjusted (by age) beta-band power and HR changes. (e and f) The same information as in (c and d) is shown but reflecting the relationship between $\log_{10}$ transformed 20 Hz power and HR changes. Note, that there was no spatial and frequency leakage from the first 10 Hz stimulus flicker harmonic at 20 Hz to the induced beta-band power changes just below 20 Hz

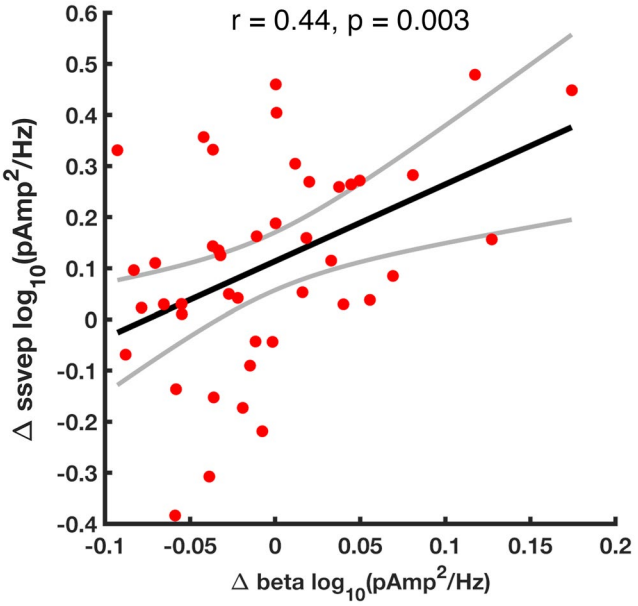

FIGURE 7 Scatterplots of adjusted mean $\log_{10}$ transformed beta-band power changes in relation to adjusted $\log_{10}$ transformed mean ssVEF power changes across the source vertices of the minimum t values for the left and right clusters (see Figures 6 and 7) are shown. The red dots represent individual data points. The black line indicates the slope, whereas the grey lines depict the 95% confidence kernel density

changes coincided with increased induced beta-band desynchronization in pre-motor and motor cortical networks reflecting enhanced excitability in motor cortical circuits. In line with our results, heightened defense responses have been associated with sympathetically driven action initiation and reduced model-based computation of environmental inputs (Mobbs et al., 2009; Obrist, 1968). This is in line with the neuro-visceral integration framework, which assumes that high threat imminence results in prefrontal hypoactivity and thus leads to a disinhibition of sympathoexcitatory circuits triggering HR acceleration and energy mobilization for prepotent fight-flight responses (Thayer & Lane, 2009).

Critically, differential neural gain control in attention and motor-relevant cortical regions were mutually related. Participants that showed increased neural gain in parietal attention networks during unpleasant picture viewing were also characterized by decreased excitability in motor circuits and vice versa. Importantly, the effects observed here cannot be explained by spatial or frequency leakage. First, linear relationships between HR changes and ssVEF power were localized in the parietal cortex, whereas beta-band associations were observed in the pre-motor and motor cortex. Due to the spatial distance between the two regions, it is unlikely that significant regression terms in both brain areas are due to spatial leakage of current source densities. Second, beta-band synchronization and desynchronization were observed just below the 20 Hz harmonic of the 10 Hz driving stimulus and induced 20 Hz power was not related to HR changes (see Figure 6e,f) safeguarding against a possible frequency leakage from the first ssVEF harmonic into the observed induced beta-band power modulations. It is also unlikely that differential eye-movement patterns can explain the observed beta-band modulations, as participants were instructed to fixate the central fixation cross throughout the experiment, and trials containing horizontal eye movements as monitored by the EOG were discarded from the analysis. Further, eye movements would have introduced orbitofrontal or prefrontal source activity at low frequencies that were not analyzed in this study.

It is also important to note that we observed the general ssVEF power modulation by emotional arousal in the visual cortex as typically reported in previous MEG and EEG studies (Hajcak et al., 2013; Keil et al., 2003, 2009; Moratti et al., 2004, 2015). However, the correlation of ssVEF power and HR change patterns for high arousing unpleasant emotional scenes was restricted clearly to parietal areas and did not overlap with the ssVEF power contrast between unpleasant and neutral pictures in more occipital brain regions. Therefore, we argue that high arousing unpleasant picture content is prioritized in the visual cortex independently of the threat imminence as indexed by physiological reactivity, whereas activity in more dorsally located parietal cortical circuits strongly covary with HR change patterns as described above.

A general increased neural gain in the visual cortex for stimuli that represent a potential danger may be a result of a prior lifelong learning experience. Thus, visual cortex activity for unpleasant emotional scenes might not be influenced by model-free versus model-based computational strategies, whereas

the modulation of the excitability of attention and motor brain circuits is bound to threat imminence. In line with this notion, Antov et al. (Antov et al., 2020) have shown that visuocortical enhancement of acquired fear-relevant stimuli returns one day after extinction learning outlasting prior peripheral responding during the initial encounter with the conditioned stimuli. Differences in perceived threat imminence as indexed by physiological reactivity may be important for the acquisition of fear-relevant visuocortical tuning processes (Moratti & Keil, 2005; Moratti et al., 2006). But once this tuning process has been consolidated, further encounters with this fear-relevant stimulus may trigger increased processing in the visual cortex independently of the current threat imminence.

In sum, parasympathetically and sympathetically dominated HR changes covaried with differential neural gain changes in attention and motor relevant brain circuits. Critically, age did not explain a significant variance of neuromagnetic activity during emotional picture viewing in these brain networks. However, at the behavioral level increased age was associated with judging unpleasant pictures as more negative than neutral pictures. This was paralleled by increased arousal rating differences between unpleasant and neutral pictures with older age. Interestingly, these age-driven differences in valence and arousal ratings were not present in HR changes to emotional pictures (there was no correlation between age and HR changes). Within healthy participants, there was also no relation between HR change and anxiety HARS and depression HDRS scores.

One of the main limitations of the present study is that we had no direct motor task. However, mental motor imagery of inhibition or execution of actions results in HR deceleration and acceleration together with changes in EEG beta-band power, respectively (Pfurtscheller et al., 2013). Therefore, an overt execution of the action is not necessary to observe these changes.

Interestingly, during the second half of stimulus presentation HR decelerators and accelerators were characterized by HR acceleration followed by deceleration, indicating that threat imminence differences as indexed by HR change emerged during the early phase of stimulus processing. However, the second part of the triphasic HR response was preserved in both groups (see Bradley, 2009; Bradley et al., 2001). Noteworthy, HR response patterns for accelerators and decelerators were similar with respect to the unpleasant subcategories of attack and mutilation scenes (see Figure S2).

In sum, the present study shows that distinct levels of threat imminence during emotional picture viewing in humans as indexed by different HR response patterns are associated with differential neural gain control in attention and motor-relevant cortical regions. This inter-subject variability in healthy participants during emotional stimulation should be taken into account in future studies that implement these paradigms for the evaluation of emotional responses in clinical samples. Further, resting-state heart rate variability measures should also be assessed in future studies, as cardiac vagal tone modulates top-down and bottom-up central processes (Park & Thayer, 2014).

ACKNOWLEDGMENTS

The current study was funded by the Spanish Ministry of Economy and Competitiveness (PSI2014-52205-R). JE was financed by a predoctoral stipend of the Complutense University of Madrid and the Santander bank. We thank Dr. Bryan Strange for his comments on this report.

ORCID

Stephan Moratti https://orcid.org/0000-0003-0824-8759

REFERENCES

Antov, M. I., Plog, E., Bierwirth, P., Keil, A., & Stockhorst, U. (2020). Visuocortical tuning to a threat-related feature persists after extinction and consolidation of conditioned fear. *Scientific Reports*, *10*(1), 3926. https://doi.org/10.1038/s41598-020-60597-z

Ashrafulla, S., Pantazis, D., Mosher, J., Hamalainen, M., Liu, B., & Leahy, R. M. (2011). Viability of Sharing MEG Data using Minimum-Norm Imaging. Medical Imaging 2011: Advanced Pacs-Based Imaging Informatics and Therapeutic Applications, 7967. https://doi.org/10.1117/12.879111

Barratt, E. L., Francis, S. T., Morris, P. G., & Brookes, M. J. (2018). Mapping the topological organisation of beta oscillations in motor cortex using MEG. *NeuroImage*, *181*, 831–844. https://doi.org/10.1016/j.neuroimage.2018.06.041

Bolles, R. C. (1970). Species-specific defense reactions and avoidance learning. *Psychological Review*, *77*, 32–48. https://doi.org/10.1037/h0028589

Bradley, M. M. (2009). Natural selective attention: Orienting and emotion. *Psychophysiology*, *46*(1), 1–11. https://doi.org/10.1111/j.1469-8986.2008.00702.x

Bradley, M. M., Codispoti, M., Cuthbert, B. N., & Lang, P. J. (2001). Emotion and motivation I: defensive and appetitive reactions in picture processing. *Emotion*, *1*(3), 276–298. https://doi.org/10.1037/1528-3542.1.3.276

Bradley, M. M., Keil, A., & Lang, P. J. (2012). Orienting and emotional perception: Facilitation, attenuation, and interference. *Frontiers in Psychology*, *3*, 493. https://doi.org/10.3389/fpsyg.2012.00493

Codispoti, M., & De Cesarei, A. (2007). Arousal and attention: Picture size and emotional reactions. *Psychophysiology*, *44*(5), 680–686. https://doi.org/10.1111/j.1469-8986.2007.00545.x

Collins, D. L., Zijdenbos, A. P., Kollokian, V., Sled, J. G., Kabani, N. J., Holmes, C. J., & Evans, A. C. (1998). Design and construction of a realistic digital brain phantom. *IEEE Transactions on Medical Imaging*, *17*(3), 463–468. https://doi.org/10.1109/42.712135

Corbetta, M., Patel, G., & Shulman, G. L. (2008). The reorienting system of the human brain: From environment to theory of mind. *Neuron*, *58*(3), 306–324. https://doi.org/10.1016/j.neuron.2008.04.017

Fanselow, M. S. (1994). Neural organization of the defensive behavior system responsible for fear. *Psychonomic Bulletin & Review*, *1*, 429–438. https://doi.org/10.3758/BF03210947

Fanselow, M. S., & Lester, L. S. (1988). A functional behavioristic approach to aversively motivated behavior: Predatory imminence as

a determinant of the topography of defensive behavior. In R. C. Bolles, & M. D. Beecher (Eds.), *Evolution and learning* (pp. 185–212). Lawrence Erlbaum Associates Inc.

Gavazzeni, J., Wiens, S., & Fischer, H. (2008). Age effects to negative arousal differ for self-report and electrodermal activity. *Psychophysiology*, *45*(1), 148–151. https://doi.org/10.1111/j.1469-8986.2007.00596.x

Graham, F. K., & Clifton, R. K. (1966). Heart-rate change as a component of the orienting response. *Psychological Bulletin*, *65*(5), 305–320. https://doi.org/10.1037/h0023258

Gramfort, A., Luessi, M., Larson, E., Engemann, D. A., Strohmeier, D., Brodbeck, C., Parkkonen, L., & Hämäläinen, M. S. (2014). MNE software for processing MEG and EEG data. *NeuroImage*, *86*, 446–460. https://doi.org/10.1016/j.neuroimage.2013.10.027

Grühn, D., & Scheibe, S. (2008). Age-related differences in valence and arousal ratings of pictures from the International Affective Picture System (IAPS): Do ratings become more extreme with age? *Behavior Research Methods*, *40*(2), 512–521. https://doi.org/10.3758/brm.40.2.512

Haagenars, M. A., Mesbah, R., & Cremers, H. (2015). Mental imagery affects subsequent autonomic defense responses. *Frontiers in Psychiatry*, *6*, 73. https://doi.org/10.3389/fpsyt.2015.00073

Hajcak, G., MacNamara, A., Foti, D., Ferri, J., & Keil, A. (2013). The dynamic allocation of attention to emotion: Simultaneous and independent evidence from the late positive potential and steady state visual evoked potentials. *Biological Psychology*, *92*(3), 447–455. https://doi.org/10.1016/j.biopsycho.2011.11.012

Hamm, A. O., & Vaitl, D. (1996). Affective learning: Awareness and aversion. *Psychophysiology*, *33*(6), 698–710. https://doi.org/10.1111/j.1469-8986.1996.tb02366.x

Hare, R. D. (1972). Cardiovascular components of orienting and defensive responses. *Psychophysiology*, *9*(6), 606–614. https://doi.org/10.1111/j.1469-8986.1972.tb00770.x

Hare, R. D., & Blevings, G. (1975). Defensive responses to phobic stimuli. *Biological Psychology*, *3*(1), 1–13. https://doi.org/10.1016/0301-0511(75)90002-2

Hermans, E. J., Henckens, M. J., Roelofs, K., & Fernandez, G. (2013). Fear bradycardia and activation of the human periaqueductal grey. *NeuroImage*, *66*, 278–287. https://doi.org/10.1016/j.neuroimage.2012.10.063

Hodes, R. L., Cook, E. W. 3rd, & Lang, P. J. (1985). Individual differences in autonomic response: Conditioned association or conditioned fear? *Psychophysiology*, *22*(5), 545–560. https://doi.org/10.1111/j.1469-8986.1985.tb01649.x

Huang, M. X., Mosher, J. C., & Leahy, R. M. (1999). A sensor-weighted overlapping-sphere head model and exhaustive head model comparison for MEG. *Physics in Medicine & Biology*, *44*(2), 423–440. https://doi.org/10.1088/0031-9155/44/2/010

Jennings, J. R., & van der Molen, M. W. (2005). Preparation for speeded action as a psychophysiological concept. *Psychological Bulletin*, *131*(3), 434–459. https://doi.org/10.1037/0033-2909.131.3.434

Jennings, J. R., van der Molen, M. W., Somsen, R. J., & Terezis, C. (1990). On the shift from anticipatory heart rate deceleration to acceleratory recovery: Revisiting the role of response factors. *Psychophysiology*, *27*(4), 385–395. https://doi.org/10.1111/j.1469-8986.1990.tb02332.x

Jennings, J. R., & Woods, C. C. (1977). Cardiac cycle time effects on performance, phasic cardiac responses, and their intercorrelation in choice reaction time. *Psychophysiology*, *14*(3), 297–307. https://doi.org/10.1111/j.1469-8986.1977.tb01179.x

Keil, A., Gruber, T., Muller, M. M., Moratti, S., Stolarova, M., Bradley, M. M., & Lang, P. J. (2003). Early modulation of visual perception by emotional arousal: Evidence from steady-state visual evoked brain potentials. *Cognitive, Affective, & Behavioural Neuroscience*, *3*(3), 195–206. https://doi.org/10.3758/CABN.3.3.195

Keil, A., Moratti, S., Sabatinelli, D., Bradley, M. M., & Lang, P. J. (2005). Additive effects of emotional content and spatial selective attention on electrocortical facilitation. *Cerebral Cortex*, *15*(8), 1187–1197. https://doi.org/10.1093/cercor/bhi001

Keil, A., Sabatinelli, D., Ding, M., Lang, P. J., Ihssen, N., & Heim, S. (2009). Re-entrant projections modulate visual cortex in affective perception: Evidence from Granger causality analysis. *Human Brain Mapping*, *30*(2), 532–540. https://doi.org/10.1002/hbm.20521

Keil, A., Smith, J. C., Wangelin, B. C., Sabatinelli, D., Bradley, M. M., & Lang, P. J. (2008). Electrocortical and electrodermal responses covary as a function of emotional arousal: A single-trial analysis. *Psychophysiology*, *45*(4), 516–523. https://doi.org/10.1111/j.1469-8986.2008.00667.x

Koelewijn, T., van Schie, H. T., Bekkering, H., Oostenveld, R., & Jensen, O. (2008). Motor-cortical beta oscillations are modulated by correctness of observed action. *NeuroImage*, *40*(2), 767–775. https://doi.org/10.1016/j.neuroimage.2007.12.018

Lacey, B. C., & Lacey, J. I. (1980). Cognitive modulation of time-dependent primary bradycardia. *Psychophysiology*, *17*(3), 209–221. https://doi.org/10.1111/j.1469-8986.1980.tb00137.x

Lachert, P., Janusek, D., Pulawski, P., Liebert, A., Milej, D., & Blinowska, K. J. (2017). Coupling of Oxy- and Deoxyhemoglobin concentrations with EEG rhythms during motor task. *Scientific Reports*, *7*(1), 15414. https://doi.org/10.1038/s41598-017-15770-2

Lang, P. J., Bradley, M. M., & Cuthbert, B. N. (1997). Motivated attention: affect, activation, and action. In P. J. Lang, R. F. Simons, & M. T. Balaban (Eds.), *Attention and orienting: Sensory and motivational processes* (pp. 97–135). Lawrence Erlbaum Associates.

Lang, P. J., Bradley, M. M., & Cuthbert, B. N. (2005). International affective picture system (IAPS): Affective ratings of pictures and instruction manual. Technical Report A-6.

Mobbs, D., Headley, D. B., Ding, W., & Dayan, P. (2020). Space, time, and fear: Survival computations along defensive circuits. *Trends in Cognitive Sciences*, *24*(3), 228–241. https://doi.org/10.1016/j.tics.2019.12.016

Mobbs, D., Marchant, J. L., Hassabis, D., Seymour, B., Tan, G., Gray, M., Petrovic, P., Dolan, R. J., & Frith, C. D. (2009). From threat to fear: The neural organization of defensive fear systems in humans. *Journal of Neuroscience*, *29*(39), 12236–12243. https://doi.org/10.1523/JNEUROSCI.2378-09.2009

Mobbs, D., Petrovic, P., Marchant, J. L., Hassabis, D., Weiskopf, N., Seymour, B., Dolan, R. J., & Frith, C. D. (2007). When fear is near: Threat imminence elicits prefrontal-periaqueductal gray shifts in humans. *Science*, *317*(5841), 1079–1083. https://doi.org/10.1126/science.1144298

Moratti, S., & Keil, A. (2005). Cortical activation during Pavlovian fear conditioning depends on heart rate response patterns: An MEG study. *Cognitive Brain Research*, *25*(2), 459–471. https://doi.org/10.1016/j.cogbrainres.2005.07.006

Moratti, S., Keil, A., & Miller, G. A. (2006). Fear but not awareness predicts enhanced sensory processing in fear conditioning. *Psychophysiology*, *43*(2), 216–226. https://doi.org/10.1111/j.1464-8986.2006.00386.x

Moratti, S., Keil, A., & Stolarova, M. (2004). Motivated attention in emotional picture processing is reflected by activity modulation in

cortical attention networks. *NeuroImage*, *21*(3), 954–964. https://doi.org/10.1016/j.neuroimage.2003.10.030

Moratti, S., Rubio, G., Campo, P., Keil, A., & Ortiz, T. (2008). Hypofunction of right temporoparietal cortex during emotional arousal in depression. *Archives of General Psychiatry*, *65*(5), 532–541. https://doi.org/10.1001/archpsyc.65.5.532

Moratti, S., Saugar, C., & Strange, B. A. (2011). Prefrontal-occipitoparietal coupling underlies late latency human neuronal responses to emotion. *Journal of Neuroscience*, *31*(47), 17278–17286. https://doi.org/10.1523/JNEUROSCI.2917-11.2011

Moratti, S., Strange, B., & Rubio, G. (2015). Emotional arousal modulation of right temporoparietal cortex in depression depends on parental depression status in women: First evidence. *Journal of Affective Disorders*, *178*, 79–87. https://doi.org/10.1016/j.jad.2015.02.031

Nichols, T. E., & Holmes, A. P. (2002). Nonparametric permutation tests for functional neuroimaging: A primer with examples. *Human Brain Mapping*, *15*(1), 1–25. https://doi.org/10.1002/hbm.1058

Obrist, P. A. (1968). Heart rate and somatic-motor coupling during classical aversive conditioning in humans. *Journal of Experimental Psychology*, *77*(2), 180–193. https://doi.org/10.1037/h0025814

Park, G., & Thayer, J. F. (2014). From the heart to the mind. Cardiac vagal tone modulates top-down and bottom-up visual perception and attention to emotional stimuli. *Frontiers in Psychology*, *1*(5), 278. https://doi.org/10.3389/fpsyg.2014.00278

Park, H. D., Bernasconi, F., Salomon, R., Tallon-Baudry, C., Spinelli, L., Seeck, M., Schaller, K., & Blanke, O. (2018). Neural sources and underlying mechanisms of neural responses to heartbeats, and their role in bodily self-consciousness: An intracranial EEG study. *Cerebral Cortex*, *28*, 2351–2364. https://doi.org/10.1093/cercor/bhx136

Park, H., Kim, J. S., & Chung, C. K. (2013). Differential beta-band event-related desynchronization during categorical action sequence planning. *PLoS One*, *8*(3), e59544. https://doi.org/10.1371/journal.pone.0059544

Perakakis, P., Joffily, M., Taylor, M., Guerra, P., & Vila, J. (2010). KARDIA: A Matlab software for the analysis of cardiac interbeat intervals. *Computer Methods and Programs in Biomedicine*, *98*(1), 83–89. https://doi.org/10.1016/j.cmpb.2009.10.002

Perusini, J. N., & Fanselow, M. S. (2015). Neurobehavioral perspectives on the distinction between fear and anxiety. *Learning & Memory*, *22*(9), 417–425. https://doi.org/10.1101/lm.039180.115

Pfurtscheller, G., & Aranibar, A. (1979). Evaluation of event-related desynchronization (ERD) preceding and following voluntary self-paced movement. *Electroencephalography and Clinical Neurophysiology*, *46*(2), 138–146. https://doi.org/10.1016/0013-4694(79)90063-4

Pfurtscheller, G., & Lopes da Silva, F. H. (1999). Event-related EEG/MEG synchronization and desynchronization: Basic principles. *Clinical Neurophysiology*, *110*(11), 1842–1857. https://doi.org/10.1016/s1388-2457(99)00141-8

Pourtois, G., Schwartz, S., Seghier, M. L., Lazeyras, F., & Vuilleumier, P. (2006). Neural systems for orienting attention to the location of threat signals: An event-related fMRI study. *NeuroImage*, *31*(2), 920–933. https://doi.org/10.1016/j.neuroimage.2005.12.034

Pfurtscheller, G., Solis-Escalante, T., Barry, R. J., Klobassa, D. S., Neuper, C., & Muller-Putz, G. R. (2013). Brisk heart rate and EEG changes during execution and withholding of cue-paced foot motor imagery. *Front Hum Neurosci*, *7*, 379. https://doi.org/10.3389/fnhum.2013.00379.

Reyes del Paso, G. A., & Vila, J. (1998). The continuing problem of incorrect heart rate estimation in psychophysiological studies: An off-line solution for cardiotachometer users. *Biological Psychology*, *48*(3), 269–279. https://doi.org/10.1016/s0301-0511(98)00039-8

Roelofs, K. (2017). Freeze for action: Neurobiological mechanisms in animal and human freezing. *Philosophical Transactions of the Royal Society B-Biological Sciences*, *372*(1718), https://doi.org/10.1098/rstb.2016.0206

Rossiter, H. E., Davis, E. M., Clark, E. V., Boudrias, M. H., & Ward, N. S. (2014). Beta oscillations reflect changes in motor cortex inhibition in healthy ageing. *NeuroImage*, *91*, 360–365. https://doi.org/10.1016/j.neuroimage.2014.01.012

Rössler, L., & Gamer, M. (2019). Freezing of gaze during action preparation under threat imminence. *Scientific Reports*, *9*(1), 17215. https://doi.org/10.1038/s41598-019-53683-4

Sagaspe, P., Schwartz, S., & Vuilleumier, P. (2011). Fear and stop: A role for the amygdala in motor inhibition by emotional signals. *NeuroImage*, *55*(4), 1825–1835. https://doi.org/10.1016/j.neuroimage.2011.01.027

Sanchez-Navarro, J. P., Martinez-Selva, J. M., Maldonado, E. F., Carrillo-Verdejo, E., Pineda, S., & Torrente, G. (2018). Autonomic reactivity in blood-injection-injury and snake phobia. *Journal of Psychosomatic Research*, *115*, 117–124. https://doi.org/10.1016/j.jpsychores.2018.10.018

Schwerdtfeger, A. R., Schwarz, G., Pfurtscheller, K., Thayer, J. F., Jarczok, M. N., & Pfurtscheller, G. (2020). *Clinical Neurophysiology*, *131*, 676–693. https://doi.org/10.1016/j.clinph.2019.11.013

Sokolov, E. N. (1963). *Perception and the conditioned reflex*. Pergamon.

Tadel, F., Baillet, S., Mosher, J. C., Pantazis, D., & Leahy, R. M. (2011). Brainstorm: A user-friendly application for MEG/EEG analysis. *Computational Intelligence and Neuroscience*, *2011*, 879716. https://doi.org/10.1155/2011/879716

Thayer, J. F. (2006). On the importance of inhibition: Central and peripheral manifestations of nonlinear inhibitory processes in neural systems. *Dose-Response*, *4*(1), 2–21. https://doi.org/10.2203/dose-response.004.01.002.Thayer

Thayer, J. F., & Lane, R. D. (2009). Claude Bernard and the heart-brain connection: Further elaboration of a model of neurovisceral integration. *Neuroscience and Biobehavioral Reviews*, *33*, 81–88. https://doi.org/10.1016/j.neubiorev.2008.08.004

Tumati, S., Paulus, M. P., & Northoff, G. (2021). Out-of-step: Brain-heart desynchronization in anxiety disorders. *Molecular Psychiatry*. Epub ahead of print. https://doi.org/10.1038/s41380-021-01029-w

Tzagarakis, C., West, S., & Pellizzer, G. (2015). Brain oscillatory activity during motor preparation: Effect of directional uncertainty on beta, but not alpha, frequency band. *Frontiers in Neuroscience*, *9*, 246. https://doi.org/10.3389/fnins.2015.00246

Vieira, J. B., Schellhaas, S., Enström, E., & Olsson, A. (2020). Help or flight? Increased threat imminence promotes defensive helping in humans. *Proceedings of the Royal Society B: Biological Sciences*, *287*(1933), 20201473. https://doi.org/10.1098/rspb.2020.1473

Weerts, T. C., & Lang, P. J. (1978). Psychophysiology of fear imagery – Differences between focal phobia and social performance anxiety. *Journal of Consulting and Clinical Psychology*, *46*(5), 1157–1159. https://doi.org/10.1037/0022-006x.46.5.1157

Yuan, M., Gimenez-Fernandez, T., Mendez-Bertolo, C., & Moratti, S. (2018). Ultrafast cortical gain adaptation in the human brain by trial-to-trial changes of associative strength in fear learning. *Journal of*

Neuroscience, *38*(38), 8262–8276. https://doi.org/10.1523/JNEUROSCI.0977-18.2018

SUPPORTING INFORMATION

Additional Supporting Information may be found online in the Supporting Information section.

How to cite this article: de Echegaray J, Moratti S. Threat imminence modulates neural gain in attention and motor relevant brain circuits in humans. *Psychophysiology*. 2021;58:e13849. https://doi.org/10.1111/psyp.13849